EXPERIMENTAL STUDIES ON INTERFACIAL BOND STRENGTH IN GFRP SYSTEMS

A Thesis Submitted
In Partial Fulfilment of the Requirements
for the Degree of
MASTER OF TECHNOLOGY

By
SRIKANTA BANDYOPADHYAY

to the

INTERDEPARTMENTAL PROGRAMME IN MATERIALS SCIENCE
INDIAN INSTITUTE OF TECHNOLOGY KANPUR
AUGUST 1973

Certificate

Certified that the work "Experimental Studies on Interfacial Bond-strength in GFRP systems" has been carried out by Mr. Srikanta Bandyopadhyay under my supervision and that this work has not been submitted elsewhere for a degree.

P. N. Murthy

(P.N. Murthy)
Professor
Aeronautical Engineering Department
Indian Institute of Technology,
Kanpur

IPMS-1973-M-BAN-Exp

ACKNOWLEDGEMENT

The undersigned greatly acknowledges the invaluable guidance and encouragement by Prof. P.N. Murthy throughout this work.

Thanks are due to Dr. M.K. Mukherjee, Head, Materials and Quality Control Division, Vikram Sarabhai Space Centre, Trivandrum for his encouragement and also for the glass fibre and resin given by him for this experimentation. Also thanks are due to Dr. E.C. Subbarao for his encouragement and appreciation

The technical help by Mr. Krishnamurthy, Mr. Pandey are acknowledged.

Heartfelt thanks are due to Mr. Kamalaksha Sarkar for frequent discussions and valuable suggestions on the work.

The neat typing by Mr. S.Kumar and drawing of figures by Debasis Mukherjee are gratefully appreciated.

Last but not the least, the author wishes to thank his wife, Nina for all the encouragement and cheers given by her.

(S. Bandyopadhyay)

SYNOPSIS

The role of fibre-matrix interface in glass-fibre reinforced plastics (GFRP) has been outlined; the previous experimental works employing pull-out technique have been surveyed and various models for determination of interfacial shear stress including that of Lawrence have been presented. The present investigation aims at experimental determination of the interfacial shear stress in a GFRP system embedding 30 end E-glass roving in polyester resin under different curing schedules. The test configuration used for this is a modification of the previous models having distinct advantages of being a realistic one and eliminating any shear stress concentration that are invariably presented but are not taken into consideration in the previous models. The schedule of operations for the specimen preparations has been suitably elaborated. Besides studying debonding and pull-out under tensile loading experiments have also been carried out under cyclic loading within the experimental range. The debonding/pull-out life increased with decreasing stress amplitude. The shear stress range for fatigue debonding has been found to be much less than that by tension-compression fatigue debonding by previous investigators. Also a mathematical expression has been developed for determination of the actual shear surface area for the multiple fibres from the projected rectangular area of the pull-out surface.

CONTENTS

SYMBOLS AND ABBREVIATIONS

Unless otherwise mentioned, following is the list of symbols and abbreviations:

A_f	Area of fibre
A_m	Area of matrix
d	Diameter of fibre
l	Length of embedded fibre
l_c	Critical length of fibre
μ	Coefficient of friction
p	Radial pressure acting on a glass fibre
σ_f	Stress in fibre
σ_m	Stress in matrix
t	Thickness
τ_{av}	Average shear stress over the embedded length of fibre
τ_i	Frictional shear stress
τ_{max}	Maximum shear stress
G_m	Shear modulus of matrix
K	Constant
e_f	Virtual fibre strain
e_m	Virtual matrix strain
γ	Work of fracture
E_f	Mod. of elasticity of fiber
E_m	Mod. of elasticity of matrix

r_o Mean distance of separation of fibres normal to their lengths. For the one fibre model system it is taken as the radius or half the width of the matrix.

u Virtual displacement of a point in the direction of the fibre at a distance x, from embedded end, if the elastic properties of fibre and matrix were identical.

v Displacement of the matrix in the same point, if the fibre was replaced by matrix.

P_{f-max} Maximum load on fibre required to achieve complete debonding and pull-out

P_f^{∞} Load required to debond an infinitely long fibre.

CHAPTER 1
INTRODUCTION AND LITERATURE SURVEY

1.1 Significance of Interface in Glass-fibre Reinforced Composites

The glass-fibre reinforced plastics composites constitute the group of materials with very high strength-to-weight ratio over a wide temperature range. These materials find great use, among others, in Aerospace applications, pressure vessels etc. When glass-fibres are embedded in a resin matrix, the high flaw sensitivity of the fibres is reduced and it is possible to utilise their high strengths for many structural purposes which is not otherwise possible. The load transfer between the matrix and the fibres takes place through interface; in case of failure of the weaker fibres, the load is redistributed through the matrix to other fibres without failure of the composite material as such.

The fibre-matrix interface in fibre-reinforced composite has a tremendous influence on the mechanical properties of the composite. To obtain optimum utilisation of the fibre-strength, the aspect ratio of the fibres (i.e. l/d) needs to be higher than the ratio of the tensile strength to the fibre-matrix interfacial strength (1). However, with strong fibres and strong interfacial bonding, it is not necessary to impose this restriction; on the other hand, an early failure of the interface, i.e. debonding gives high fracture toughness in fibre-reinforced composites (2, 3, 4). The role of interfacial bonding on the efficiency of

reinforcement has been analysed theoretically by Krenchel (5) for linear, planar and random types of reinforcement.

Agarwal (6,7) has considered different values of the interface properties (Young's modulus, poisson's ratio etc.) and then showed using Von Mises criterion that the strength and elastic modulus can be changed independently with interface properties. Also, since a high modulus for interface means a high degree of stress transfer, the effective strength and elastic modulus of composite increase, thus giving a low value of ultimate elongation, thereby giving a low impact. He has shown that an optimisation of toughness, elastic modulus and strength can be made by controlling the interface properties.

1.2 Previous Work

The glass-resin joint strength specimens used thus far can be categorised (8) as i) flat-plate specimens and ii) rod or fiber-bond strength specimens, of which the latter type appears to have advantages in that geometrically they are more similar to actual glass resin composites, residual stresses produced in specimens due to resin curing are similar to those in actual composites and the initiation of failure in them is more realistic (8).

While considerable work has been carried out to determine the bond strength of G.F.R.P. by various methods, the importance of the fibre pull-out (which is directly influenced by the

development of fibre-matrix interfacial bond strength) has not been sufficiently emphasised. Very little theoretical and experimental work have been done to determine the glass-resin interfacial shear strength by fibre pull-out method. Cottrell (9) gave a theoretical model to analyse the fibre pull-out from a ductile matrix in which a shear stress is developed along the axis of the fibres by plastic deformation of the matrix material. However, he has not taken into account the interaction between fibres. Cooper (10) studied pull-out of fibres from matrix under bending as well as tension tests of notched fibrous composites. Glass-rod specimens have been used for measurement of interfacial shear by pushing or pulling the rod (which is from 1 to 1 mm in diameter) through a resin disc cast around a small part of the rod (11). Figure 1 (12) gives a typical curve for such a test. The bond strength was determined by dividing the peak bond load by the bond surface area. However, apart from the peak debonding load, Figure 1 also shows the presence of considerable frictional force, after debonding, that comes as a result of the resin shrinkage. deVekey and Mazumdar (13) employed the pull-out method for determining the interfacial shear strength for various combinations of fibres and matrices where they had embedded E-glass rods 0.5 to 1.0 mm in diameter, perpendicularly in a matrix contained in a special mould and stressed the rod in tension. The value of the maximum bond load corresponded to a sharp peak in the load-extension curve.

1.3 Scope of the Present Work

The present work investigates the gross interfacial shear strength of a composite system involving a bundle of E-glass fibres in polyster resin. Apart from carrying out the debonding/pull-out tests in tension, the same has been carried out under cyclic loading. The 30 end E-glass roving which was used as the bundle of fibres, constituted 'densely packed fibres' in the resin. The purpose of this was to simulate the actual conditions in a composite, where multiple strands or bundles are used as reinforcement, as, for example, in a filament wound composite. Also, while testing the strength of the fibre bundles unimpregnated by resin, the fibres appeared to undergo 'supercreep', after crossing the ultimate load, at a low but consistent load of 0.5 Kg with about 100 percent total elongation of the original length during the creep.

1.4 Previous Models and Theoretical Analyses for Determination of Interfacial Shear Strength

Various theories have been proposed for the longitudinal stress distribution in the fibre and also the interfacial shear developed in a discontinuous fibre reinforced composite. Of these, the model suggested by Dow (14) has some good relevance to pull-out mechanism. Also, outwater's concept (15) of the frictional component of the radial force on the glass fibre by the surrounding 'thin' resin tube caused by resin shrinkage on curing

physically explains how stress transfer could still take place through the interface even after debonding has taken place.

In his model, Dow (14) assumed that perfect bonding exists between fibre and resin and that straight lines before deformation are straight after deformation. Considering an element of fibre and of the matrix at the interface, the equilibrium equations become, for a load being applied to the matrix as shown in Figure 2:

Fibre element: $$\tau_J = -\frac{1}{2\pi r_f}\frac{dF_f}{dz} \qquad (1)$$

Matrix: $$\tau_J = \frac{1}{2\pi r_f}\frac{dF_m}{dz} \qquad (2)$$

A similar analysis given by Cox (16) for a three dimensional model shows the variation of shear stress along the length of a fibre in Figure 3, where l_c = critical length of fibre. He had assumed a perfect fibre-matrix bonding and equal lateral contraction of fibre and matrix (i.e. no load transfer through the end of the fibre).

Outwater considered a low bond strength between fibre and matrix, which is usually the case with fibre-reinforced plastics. He assumed that 1) The fibres carry the entire load, 2) the matrix film surrounding the fibres is of negligible thickness.

Upon considering these films to be very thin, he considered that when they shrink on to the fibre, they become highly

stressed, the upper limit of the stress being the yield stress of the matrix σ_y. The radial pressure, p, acting on the fibre was calculated as, from Figure 4,

$$p = -\frac{\sigma_y t}{2r_f} \qquad (3)$$

The frictional component of this radial pressure will be resisting any relative movement between the matrix and the fibre. If we consider virtual displacements, then, from Figure 5,

$$\frac{d\sigma_f}{dx} dx \pi r_f^2 = -\mu p \; 2\pi r_f \, dx \qquad (4)$$

where μp is the frictional shear stress. Integrating,

$$(\sigma_f)_c^x = \frac{\mu \sigma_y t x}{r_f^2} + c \qquad (5)$$

The constant of integration, c, can be shown to be zero by considering adhesion at the end of the fibre to be zero, for a discontinuous fibre. Thus,

$$\sigma_f = \frac{\mu \sigma_y t x}{r_f^2} \qquad (6)$$

In his theoretical model for a ductile matrix with a bundle of parallel elastic fibres, strained longitudinally, Cottrell (9) considered a tangential stress exerted on a fibre by the yielding matrix and found out the stress $\sigma(x)$ in the fibre at a distance x from one end of them, for a fibre radius r_f,

$$\sigma(x) = 2\tau x / r_f \qquad (7)$$

He found the critical length l_c to be as follows:

$$l_c = r_f \sigma_f / 2\tau$$

where σ_f = fracture stress of the fibre. For $l < l_c$, the fibres, instead of breaking will be pulled out of their holes. Assuming the tangential shear stress to be continuously exerted during the pull-out the work of fracture of order

$$2\gamma = (A_f \tau / 3r_f)\,(l/2)^2$$

le expected.

or, $$2\gamma = \frac{A_f \tau l^2}{12 r_f} \qquad (8)$$

In the model described in Figure 1, the established relationship for interfacial shear stress is as follows:

$$\tau = \frac{P_{max}}{2\pi r_f l} = \frac{\sigma_{max}\, r_f}{2l}$$

for a single rod, assuming a uniformally distributed shear stress along the interface. It appears from this that the embedded rod length will be influenced by the rod strength so that the maximum embedded length which can be used is given by

$$l = \frac{\sigma_{ult}\, r_f}{2} \qquad \sigma_{ult} = \text{ultimate strength of fibre}$$

If the embedded length is greater than that predicted by this equation, then the rod will fail in tension before pull-out occurs

In their work, deVekey and Mazumdar (13) employed the plastic-matrix theory, which assumes a uniform shear strength along the length of the embedded fibre, which, to a close approximation, may be considered for fibre pull-out from an elastic matrix with short fibres.

The main difference between the elastic matrix and plastic matrix is that in the former case the shear stress is no longer uniform and also that the variation of load transfer between fibre and matrix along the length of the fibre is not uniform. In his equation for the shear-stress along fibre-matrix interface, Gresczuk has (17) considered fibre pull-out assuming an effective interface width.

Lawrence (18) has dealt with the case of fibre pull-out in elastic matrix. Whether debonding and pull-out will occur will depend on the maximum shear stress developed relative to the shear strength of the fibre-matrix interface. He has also determined the variation in load necessary to consider fibre pull-out and in the maximum shear stress developed for various length of embedded fibres.

The geometry of fibre pull-out test for a single fibre, employed by Lawrence is shown in Figure 6. With an axial load P_f applied to fibre,

$$dP = c\,\tau(x)\,dx \qquad (9)$$

where dP = change in load P at x, along the fibre and $\tau(x)$ is

the shear stress function in terms of x and c is the circumference of the fibre in contact with the matrix.

$$\tau = K\,(u-v) \tag{10}$$

where K is a constant i.e. (u-v) is the slip.

$$dP = c\,K\,(u-v)\,dx \tag{11}$$

or
$$\frac{dP}{dx} = H\,(u-v) \tag{12}$$

where $H = c\,K$.

Cox gave the value of H as

$$H = \frac{2\pi\, G_m}{\ln\,(r_o/r_f)}$$

Differentiating (12)

$$\frac{d^2P}{dx^2} = H\,\left(\frac{du}{dx} - \frac{dv}{dx}\right) = H\,(e_f - e_m) \tag{14}$$

where e_f, e_m are the virtual fibre and matrix strains respectively at point x.

or,
$$\frac{d^2P}{dx^2} = HP\left(\frac{1}{A_f\,E_f} - \frac{1}{A_m\,E_m}\right) \tag{15}$$

$$= \frac{HP}{R} \tag{16}$$

where $1/R = \dfrac{1}{A_f\,E_f} - \dfrac{1}{A_m\,E_m}$.

Putting H/R = a

we can get a solution for equation (16) as

$$P = P_f\,\frac{\text{Sinh}\,\sqrt{a}\,x}{\text{Sinh}\,\sqrt{a}\,l/2} \tag{17}$$

It can be seen that for short embedded fibre i.e. small l/2, the build up of the load along the fibre length is approximately linear, which is not, however, the case for a long embedded fibre.

The distribution of shear stress along the fibre length (18)

Now, $\tau = K(u-v)$ or, $\frac{d\tau}{dx} = \frac{KP}{R}$

or $$\tau = \frac{K P_f \ \text{Cosh} \sqrt{a}\, x}{R \sqrt{a} \ \text{Sinh} \sqrt{a}\, l/2} \qquad (18)$$

The maximum shear stress occurs when Cosh $\sqrt{a}$ x is a maximum, i.e. at x = l/2 i.e. the point where the fibre enters the matrix.

Hence,

$$\tau_{max} = \frac{K P_f \ \text{Coth} \sqrt{a}\, l/2}{R \sqrt{a}} \qquad (19)$$

Load to pull-out and the determination of the shear strength (18)

a) Variation of the embedded fibre load to pull-out with embedded fibre length (18)

$$\tau_{max} = \frac{K P_f}{R\sqrt{a}} \ \text{Coth} \sqrt{a}\, l/2$$

Now, this being the maximum shear stress along the embedded fibre length, for a certain P_f such that τ_{max} equals the shear strength of the interface then the fibre will debond from the matrix at the point where the fibre enters the matrix.

After debonding occurs, whether the fibre continues to debond at a constant P_f of whether an increase in load is still necessary, depends upon a number of factors.

Let the length of debonded zone be $(1/2 - x)$ under the load P_f. Then, at the bonded/debonded interface the load in the fibre is given by $P_f' = P_f - \tau_i c (1/2 - x)$ and it is assumed that τ_i is constant over the debonded region.

The shear stress at the corresponding point will be

$$\tau = \frac{K P_f'}{R\sqrt{a}} \operatorname{Coth} \sqrt{a}\, x \qquad (20)$$

Now, if, as more and more debonding occurs i.e. as x decreases this expression is always equal to τ_s, then debonding will continue, if decrease in P_f' be compensated by the increase in the term $\operatorname{Coth} \sqrt{a}\, x$ as x decreases.

Then $P_f' = P_f - \tau_i c (1/2 - x)$

$$= \tau_s \frac{R\sqrt{a}}{K} \tanh \sqrt{a}\, x \qquad (21)$$

Differentiating this and putting $\frac{dP}{dx} = 0$ for maximum load, we get

$$x = x_{max} = \frac{1}{\sqrt{a}} \operatorname{Cosh}^{-1} \sqrt{\tau_s / \tau_i} \qquad (22)$$

Debonding will continue at this point without any further increase in P_f with catastrophic bond failure. Clearly the stage at which debonding becomes catastrophic is dependent

on the ratio τ_s / τ_i

For $\tau_s / \tau_i \geq \text{Cosh}^2 \sqrt{a}\, 1/2$, for $x_{max} = 1/2$, the debonding process is catastrophic immediately after it commences. For $\tau_s / \tau_i < \text{Cosh}^2 \sqrt{a}\, 1/2$, a further increase in P_f will be necessary for debonding to continue.

The maximum load on the fibre for complete debonding and pull-out is given by

$$P_{f\max} = \frac{\tau_s R \sqrt{a}}{K} \tanh \sqrt{a}\, 1/2 \quad \text{for} \quad 1/2 \leq x_{max}$$

$$= \frac{\tau_s R \sqrt{a}}{K} \tanh \sqrt{a}\, x_{max} + \tau_i c\, (1/2 - x_{max})$$

$$\text{for } 1/2 > x_{max} \qquad (23)$$

It is assumed that $P_{f\text{-}max}$ is less than the breaking load of the fibre, and pull-out and not fibre fracture occurs. Once debonding has completed and pull-out has commenced the load will fall to a value $\tau_i c\, 1/2$ and continue to fall as the fibre is withdrawn.

Gresczuk (17) considers only the immediate catastrophic failure of the interfacial bond and assumes that all the fibre load is transferred to the matrix by shear faces with no frictional force present. This requires that $\tau_i = 0$, so that from equation (23), the maximum load to pull-out being given by the expression:

$$P_{fo\,max} = P_f^{\infty} \tanh \sqrt{a}\, l/2$$

This is identical with $\tau_i = 0$, a particular case of the more general equation for $P_{f\text{-}max}$ when $l/2 \leq x_{max}$ and catastrophic failure always occurs.

b) <u>The variation of maximum shear stress with embedded fibre length and determination of the shear strength from a pull-out test (18)</u>

$$\tau_{max} = (K P_f / R \sqrt{a}) \operatorname{Coth} \sqrt{a}\, l/2$$

Also, $$\tau_{max} = \tau_{max}^{\infty} \operatorname{Coth} \sqrt{a}\, l/2$$

where $$\tau_{max}^{\infty} = K P_f / R \sqrt{a}$$

If the fibre has debonded to an effective bonded length $l'/2$, then

$$\tau_{max} = \frac{K P_f'}{R \sqrt{a}} \operatorname{Coth} \sqrt{a}\, l'/2 \qquad (24)$$

For very short fibres or for long fibres after substantial debonding has shortened the effective embedded length, the shear stress at the point where the fibre 'enters' the matrix can be very large compared to that in case of infinite fibre length for low friction condition.

$$\tau_s = P_f^{\infty} \sqrt{a}/c \; ; \quad P_{f max} = \tau_s \frac{R\sqrt{a}}{K} \tanh \sqrt{a}\, l/2 \qquad (25)$$

Gresøzuk (17) examined the trend of $P_{f\text{-}max}$ at short embedded fibre lengths and extrapolated to zero embedded fibre length. Again, the equation (25) is

$$P_{f\text{-}max} = \tau_s \frac{R\sqrt{a}}{K} \tanh \sqrt{a}\, l/2$$

Now as $\sqrt{a}\, l/2$ tends to 0 then $\tanh \sqrt{a}\, l/2$ tends to $\sqrt{a}\, l/2$. Thus τ_s tends to $P_{f\,max}/c\ l/2$ i.e. τ_s tends to τ_{av}, Where τ_{av} is the shear stress obtained by dividing the load by the total interfacial area.

1.5 Present Approach - Proposed Model

The model, as shown in Figure 7 employs a glass roving embedded through and through in a resin matrix. The length of embeddment being short, approximation for short fibres viz. $\tau_s \rightarrow \tau_{av}$ has been used for determination of the average shear strength.

The other distinct advantages over the existing models are:-

i) It is a realistic one, in the sense that in most of the applications like pressure vessel, filament wound rocket motors, multiple strand-composites are used.

ii) The stress concentration that will arise because of discontinuity at the end of the fibre in Lawrence and

Greszczuk models has been eliminated by embedding the roving completely in the matrix. In the latter models, the maximum shear stress will be developed at the point where the fibres enter the matrix when the maximum shear stress exceeds the interfacial shear stress, debonding will initiate and then it will propagate along the length of the fibre. If, in actual case, because of stress concentration near the end of the fibre, a shear stress of magnitude higher than τ_s is developed earlier, debonding may initiate there. Recently Rao, Patil and Raju (19) have given a finite element solution for stress concentration around the discontinuous fibre end.

In the proposed model, by eliminating the stress concentration and also maintaining the boundary conditions, viz. $P_f = P_{f\text{-}max}$ at the fiber entering point and $P_f = 0$ at the embedded end, has been made quite simple and easily and more appropriately applicable to pull-out systems employing even longer embedded fibres.

CHAPTER 2

EXPERIMENTAL PROCEDURE AND OBSERVATIONS

2.1 Experimental Procedure

In the present investigation, E-glass fiber roving has been embedded in polyester resin as the pull-out specimen. The specimen designed for pull-out test is shown in Figure 7. The advantages of this system are:

a) easy to fabricate.

b) No stress concentration is introduced as may be introduced by the fabrication method in a discontinuous fibre composite system.

c) No stress concentration because of geometrical discontinuity at the end of the glass fibres.

d) The load at the fibre end being zero, Lawrence's analysis can be employed.

However, the assumptions are that:

i) Normal stresses at the outer fibre-matrix interface are insignificant and debonding and pull-out is only influenced by shear stresses developed along the interface.

ii) Compressive forces that may be introduced by the grip are neglected.

30-end E-glass roving of the following specifications has been used as the reinforcement material by using a single strand.

Diameter of individual fibre	: 0.00035 inch (average)
No. of fibres per roving	: 204
No. of rovings	: 30
Coupling agent	: Silane

The polyester resin, of M/s. Hylam Ltd., Hyderabad, India was used in as supplied condition, without any dilution, as the matrix material. 1.25 percent each of MEK peroxide and Cobalt Napthanate was used as catalyst and accelerator respectively. The parting agent was supplied by CIBA.

Cylindrical split mold (Plate 1) of internal diameter 3/8" were made by axially cutting a brass tube of 3/8" i.d. and then internally grinding. The length of the cylindrical molds were 1.25 inch.

2.1.1 Preparation of the Specimens

Following was the schedule of operations for making the specimens:

2.1.1.1 Fixing of roving in the mold cavity

1. Clean the molds; clean the molding table platform (Plate 2).
2. Apply mold release agent to the mold cavity and parting lines, the portion of the table surrounding the hole and also the hole itself.

3. Allow the mold release agent to dry; repeat operation 2 two times upon drying after each application.

4. Close one pair of the matching parting lines with plastison clay so that the mold can be opened about the other parting line to encircle the fibres without touching them.

5. Cut a desired length of roving and fix it on one side with the stand (Plate 3) through the hole in it. The bottom end of the fibre is passed through the hole of the table platform and fixed with the lower side of the platform so as to keep in slight tension. Precaution should be taken that the fibre strands in the specimen portion do not touch any abrasing surface. Also, there should be no twist upon the fibre.

6. Encircle the roving by the mold as mentioned in step (4).

7. Place the mold on the table and any possible leakage is prevented by sealing

8. Seal the remaining pair of parting lines and then adjust for centering by viewing through the hole in the stand and the hole in the table platform.

Plate (5) gives an assembly of the mold ready for casting.

2.1.1.2 Preparation of Resin

The parent resin was preserved in a Refrigerator so as to prevent any deterioration with time. The following was the composition of resin mixture to embed the roving.

Catalyst : MEK peroxide : 1.25%

Accelerator : Cobalt Napthanate : 1.25%.

No diluting agent was added to the resin.

The sequence for preparation of resin mixture is as follows:

1) Add accelerator to the parent resin in a plastic container with spout; stir carefully with the specially made stirrer (Plate 6) so as to avoid vortex formation and thus minimising entrapping of air.
2) Add the hardener and mix carefully as above.
3) Keep the resin mixture in an evacuated chamber (Plate 7) for a period not exceeding five minutes whereby any bubble entrapped is easily driven out.
4) Take the mixture out of the evacuated chamber and pour slowly and carefully into the mold cavity. Since the hole on the table platform is also sealed after fixing the fiber, the resin cannot leak. The pouring was done essentially under atmospheric pressure.

2.1.1.3 After-Pouring Operation

1) The assembly is allowed to rest undisturbed for predetermined periods of time during which curing takes place.
2) After curing, release the top end of the roving from the stand. Take the mold off the table and strip.

The above operations of casting are then carried out for casting the other end of the roving.

The bond strength determination was carried out with the portion cast first, because it is only in this portion the roving is exposed to atmosphere for a very short period, not exceeding a few minutes, before casting.

It needs to be mentioned that the bulk of the roving should be kept in a dehydrated chamber to avoid attack of fibres by moisture (Plate 9).

The end to be tested for debonding is cut to various small size, the thickness of the disc varying from 3 to 5 mm and the end finely ground; while this end serves the purpose of the debonding specimen the other end of the casting essentially serves as a grip, However, the thickness of the latter is always kept considerably higher than the test end for obvious reasons.

While some specimens were tested without impregnation of the fibres in between two cast ends, in most of the specimens, the fibres were impregnated with resin for reasons explained below.

Plate (8) shows a specimen ready for pull-out test with impregnation.

In a case where it was necessary to cure the resin at temperatures higher than room temperature, the operation of casting was carried out inside an oven of internal dimensions 2 ft x 2 ft x 3 ft.

2.1.2 Testing of the Specimen

The specimens were tested in an Instron machine (5 tons) in the load range of 0-100 Kg - high sensitivity. The two ends were held in the grips (0.281-0.500" cylindrical Instron grips) and loaded slowly in tension at different rates of cross head movement. The matrix was loaded normally through the grips and through the interface the load was transferred to the fibers. The criterion for pull-out was selected such that no resin would appear sticking to the debonded and pulled out surface of the roving when seen by unaided eye.

Apart from loading in tension tests were also carried out to study the debonding and pull-out under low-cycle fatigue loading using fluctuating tension.

2.2 Observations

2.2.1 Pull-out tests without impregnation of the fibres

i) No pull-out was observed;

ii) Bulging of the fibres took place;

iii) There was a surprisingly significant amount of extension of the fibers prior to physical separation at a constant load, very near to zero.

The load-displacement curve for fibers without impregnation is shown in Figure 8. As the load started rising, at a load much less than the ultimate load, viz. about 10 Kg. significantly visible bulging of the fibers was observed that was initiated by formation of very fine and small flakes on the fibers perpendicular to the loading axis. As the load was increasing, the formation of flakes was enhanced resulting in increased bulging. Maximum bulging was observed in the central region. After crossing the ultimate load, the fibres did not physically separate, the load gradually but steeply falling down with extension of fibers occurring. When the load came to a value of 0.5 Kg (it was a distinct value and not because of any calibration error, which was checked), the fibers started elongating at this load for a long time without physical separation. After considerable elongation, the load started falling to zero very slowly and then physical separation was obtained as load fell to zero. The Plate 4 gives a picture of the bulged out fibres.

2.2.2 Pull-out tests with impregnation

Because of non-observance of debonding/pull-out by loading the fibers without any impregnation, the fibres were then given impregnation in order to eliminate the above phenomenon and thus also increase the load carrying capacity of the fibres, so as to develop the debonding shear stress.

Reproducible results of debonding and pull-out were obtained with impregnated fibre specimens. However, in some cases resin matrix fractured which was possibly due to the fact that some where in the resin very close to the interface a crack was initiated which then propagated, causing resin fracture. Also, in a few cases, where the embedded length of the fibers was large, then , before debonding shear stresses were developed along the interface, the ultimate strength of the impregnated roving was reached, as we see from Figure 1, and roving tensile failure occurred without debonding and pull-out taking place.

A set of experiments were carried out by using collets, so as to avoid compressive stresses that may be introduced in the disc by grips and at the same time reducing the disc diameter by 20% . In all the cases fracture of resin was observed, even by considerably reducing the thickness of the disc. The explanation for this could be found in the following:

i) Before the debonding shear stress was developed at the interface, some crack initiated in the resin close to the

interfacial resin, as mentioned before, and propagation of this crack fractured the resin.

ii) In case of holding the disc by grip, there was a definite amount of compressive stress that might have arrested the crack, and thereby facilitating the debonding phenomenon. However, it is suggested that a more rigorous study should be carried out to evaluate the effect of compressive stress.

The typical load-displacement curve for cases of neat debonding and pull-out is presented in Figure 9. At low load values, a grip effect is observed causing initial diversion from linearity. However, at higher load, the load-displacement curve was linear. There was a distinct value of load at which the load displacement curve again diverted from linearity, which can be termed as debonding commenced. The peak bond load was achieved shortly after that beyond which point the load started decreasing again, while pull-out was continuing. And shortly after that the load instantaneously fell to zero as the fibres were being withdrawn from the matrix

As mentioned earlier, the criterion selected for 'neat debonding and pull-out' is that no resin visibly will be sticking to the fibres - in this case, the outer fibres - when seen by unaided eye. The section from a macropoint of view appeared to be rectangular (Plate 10), since the diameter of fibres is very small. A simplified model for array of fibres and shear perimeter are shown in Figures 10 and 11.

2.2.3 Derivation of the actual shear surface from the measured (rectangular) surface

While it is easy to measure the rectangular perimeter of the surfaces, the area calculated from this will be much less than the actual area, consequently introducing an error in the value of shear stress. The following mathematical analysis, the actual shear perimeter can be observed from the observed shear perimeter.

Referring to Figure 11,

let d = dia of individual fiber

m = no. of fibres along one side

n = no. of fibres along the other side

$\bar{a}$ = average distance between two fibres, filled by resin.

p_{s_m} = measured shear perimeter

p_{s_a} = actual shear perimeter

then for unit depth,

$$p_{s_a} = 2 (m + n) d \pi/2 + 2 (m + n) \bar{a}$$

considering both the surfaces.

$$p_{s_m} = 2 (m + n) d + 2 (m + n) \bar{a}$$

The relation between p_{s_a} and p_{s_m} can be obtained as follows:

$$\frac{p_{s_a}}{p_{s_m}} = \frac{(m + n)\, d\, \pi + 2\bar{a}\, (m + n)}{2\, (m + n)\, d + 2\, (m + n)\bar{a}}$$

$$= \frac{d\pi + 2\bar{a}}{2d + 2\bar{a}}$$

Now, from microstructural study, $\bar{a}$ is found to be approximately equal to $\frac{1}{3}$ d.

Hence, $\frac{p_{s_a}}{p_{s_m}} = \frac{d\, (\pi + 2/3)}{d\, (2 + 2/3)}$

$$= \frac{\pi + 2/3}{2 + 2/3}$$

$$= \frac{3\pi + 2}{8} = 1.43$$

The average interfacial shear stress to cause debonding is given by

$$\tau_{av} = \frac{P_{f\text{-}max}}{1.43\, p_{s_m}\, l}$$

The Table 2 presents the values of the debonding shear stress obtained in the present study. The mean of five values is recorded along with the standard deviation in each case.

In low-cycle fatigue tests under fluctuating tension debonding and pull-out were observed at significantly low

cycles for high stress range. However, as the stress value was reduced, the number of cycles for debonding/pull-out considerably increased. The fatigue debonding values are presented in Figure 12.

CHAPTER 3

DISCUSSION AND CONCLUSION

3.1 Results and Interpretation

The values of the interfacial bond strengths of previous authors as well as the present work have been presented in Tables 1 and 2 respectively.

Within the experimental range of curing temperature the bond-strength increased with increased curing temperature. However, it is suggested that work should be carried out for a wider range of temperature for complete evaluation of the temperature effect.

The typical load displacement curve, corresponding to Figure 9 for the present investigation is broadly similar to those of previous authors (12)(13) viz. a chemical debonding portion followed by a mechanical debonding or frictional portion. However, the marked distinction in the nature of the curve in Figure 9 is the absence of any sharp peak, as obtained in the latter. Figure 9 shows a progressive debonding, propagation of debonding and pull-out of the roving. Deviation of the curve from linearity marks the onset of debonding which is then followed by an increase in load necessary for propagation of the debonding process. As the chemical debonding phenomenon was complete, the load values

started falling when mechanical debonding set in. The observed phenomenon of increasing load for propogation of debonding and subsequent dropping of load for mechanical or frictional debonding agree well with the theoretical analysis of Lawrence.

The area under curve shown in Figure 9 will be proportional to the total energy required (i.e. the external work done) to complete the debonding and final pull-out.

3.2 Effect of Multiple Strand

For a multi-fibre system, the load P_{max} for debonding will obviously be higher than that for a single fibre. But the increase in the load will not be in the same proportion as the number of fibres in the multiple strand because in a multiple strand the effective interfacial shear area will be much less than the area considering all the fibers individually. The breaking of some fibers because of statistical strength distribution will also have some effect.

Within the resin disc the multiple strand could be envisaged to have an outer array of fibres with an inner core. An examination of the debonded and pulled out roving shows that while debonding has taken place along the outer interface, the fibers in the core are not debonded from each other, as if the roving has behaved like a rigid system. This in general implies that the shear stress developed there was

less than the debonding shear stress or, in other words, the core fibers appeared to bear less load than the outer fibers. However, consideration should also be given to the fact that apart from the shear stress, in the core fibers, a radial tensile debonding stress will come into play (2) because of the densely packed nature there. Consequently at the core, the resulting debonding stresses will be the resultant of the shear component and the radial normal component. We may hence conclude that for this system the shear stresses developed along the outer fiber-matrix interface is higher than the resultant debonding stresses developed in the core.

A microscopic observation revcals the evidence of multiple cracks on the outer fibers. These crack tips will invariably give rise to stress concentration along the interface. This being due to the inherent nature of the statistical stress distribution of the fibers cannot be ruled out. Further, the fibers being densely packed, therewill be overlapping of stress fields, an actual assessment of which will make the thing very much complicated. Since, in the present system, short embedded fibres, not exceeding 4 mm in length are considered, we can ignore this effect, our main aim being the determination of gross or average shear strength.

3.3 Effect of Cyclic Loading

In reinforced plastics, during each cycle of loading, there takes place an appreciable amount of heat generation

which is difficult to dissipate rapidly because of the low thermal conductivity of the material.

The fatigue experiments for various systems of GFRP have indicated that there appears to exist no fatigue limit (22) which seems to be a general criterion for most fiber reinforced composites.

The main difference between the fatigue failure and tensile failure for GFRP is the difference in appearance of fracture surfaces. During fatigue failure of GFRP, the first change that takes place is the fibre-matrix debonding which takes place at values of n several order of magnitude below the failure value. Debonding is followed by resin cracking which in turn is followed by failure. Cherry (22) has indicated that fatigue lives can be specified even for the onset of debonding and resin cracking phases, as well as failure and in some applications these might be as important as actual separation of the material. Figure 12 shows the relationships between stress and number of cycles at which these processes occur. There is possible advantage of relating fatigue behaviour of glass fiber composites to strain rather than stress and it was observed that the number of cycles necessary to produce debonding depended mainly on the maximum strain, and not the type of material. Agarwal (23) observed that in crossply-composites under fluctuating tension, debonding initiated and occurred in the cross-fibers whereas in the

longitudinal fibres there was no debonding.

In the present work, the debonding aspect under cyclic loading was studied by employing a low frequency viz. 18 cycles per mt. The criterion for debonding was the pull-out of fibres from the matrix. The trend of the fatigue life with stress amplitude within the experimental limit showed the increase of fatigue debonding life with decrease in applied stress amplitude. It is suggested that this aspect be taken care in greater detail to study the mechanism as well as the S-N curve for debonding/pull-out.

However, a comparison of the debonding fatigue life presented by Cherry in Figure 12 to those in the present work (cure temperature: 45°C) reveals that while the nature of the debonding 'band' is similar in both the cases, the stress levels corresponding to a certain number of cycle in the former case is much higher than the same in the present work. The reason appearing solely to be the different fatigue mechanisms in the two cases. In the former case the debonding takes place perpendicular to the loading directions, whereas in the present work the slip is by shear. There remains a lot to investigate as to under what conditions of fatigue loading, there will be preferential debonding by either of the two mechanisms.

REFERENCES

1. M. Nicholas: 'The Strength of Metal/Alumina Interfaces'; J. Mat. Sci., 3, 571-576 (1968).

2. A. Kelley and G.T. Davis: Met. Rev. 10, 1965, 37.

3. J. Cooke and J.E. Gordon; Proc. Roy. Soc., 281A, 1964, 508.

4. A.A. Baker and D. Cratchley; Applied Research, 5, 1966, 92.

5. Krenchel, H: Fibre Reinforcement, Copenhagen, Akademisk Forlag, 1964, H-160.

6. Broutman, L.J. and Agarwal, B.D.: 'Effects of the Interface on the Mechanical Properties of Composite Materials.' Paper presented to the Sixth International Conference on Rheology, Lyon, France, Sep. 4-8, 1972.

7. Broutman, L.J. and Agarwal, B.D.; 'A Theoretical Study of the Effects of Interface on Composite Toughness', Proc. 28th Symp. S.P.I. R.P./Composites, Feb. 1973.

8. L.J. Broutman: 'Fibre-Reinforced Plastics'. Ch. 13, Modern Composite Materials, Ed. Broutman and Krock, Addison Wesley Publ.Co., 1967.

9. Cottrell, A.H: 'Strong Solids' : Proc. Roy. Soc., London, Vol. : 282A (1964) pp 2-9.

10. G.A. Cooper: 'Fracture Toughness of Composites Reinforced with Weakened Fibres'. J. Mat. Sci., Vol. 5, 1970, 645-654.

11. 'Bond Studies in Glass-reinforced Plastics'. Progress Report MCA-MIT Plastics Research Project, Plastics Research Laboratory, M.I.T.; Oct.1-1957.

12. R.D. Mooney and F.J. Megarray: 'Resin - Glass Bond Study'. Proc. 14th Conf., SPI Reinforced Plastics Divn., Feb. 1959, Section 12-E.

13. R.C. deVekey and A.J. Mazumdar: Determination of Bond Strength in Fiber-Reinforced Composite- Mag. Concrete Research. Vol.20, 1968, pp 229.

14. Hollister and Thomas: Fibre Reinforced Materials, Elsevier Publ. Co., 1966.

15. Outwater, J. Ogden, Jr.: Mod. Plastics, March, 1956, p. 56.

16. Cox, H.L.: Brit. J. Appl. Phys., 3, 72 (1952).

17. Gresczuk, L.B. in ASTM STP 452, 1969.

18. Lawrence; J. Mat. Sci., Vol. 7, No. 1, Jan. 1972.

19. A.K. Rao, S.S. Patil, I.S. Raju: Special Finite Elements for Composites, First Conference on Reinforced Plastics and their Aerospace Applications, Trivandrum, India, Aug. 1972, Session 6.

20. L.J. Broutman and F.J. Mcgarry: Mod. Plastics 40, (1962) p. 161.

21. Broutman, L.J.: ASTM STP 452, 1969.

22. Cherry, B.W. and Harrison, N.L.: The Strength and Fracture Toughness of Glass Fibre Reinforced Plastics - Applied Polymer Symp. No. 17, pp 73-94.

23. Agarwal, B.D. and Dally, J.W. : Low Cycle Behaviour of Glass Fiber Reinforced Plastics. Proc. Army Symposium on Solid Mechanics, 1970, AMMRC MS 70-5.

TABLE 1 : TYPICAL VALUE OF INTERFACIAL STRENGTH OF POLYMER-GLASS SYSTEMS

Test method	Matrix	Fibre/Glass treatment	Curing condition	Interface failure mode	Bond strength (p.s.i)	Reference
Rod-disc (push test)	Polyester cryslic 195	E-glass	24 Hr/ 40°C	Shear	750	deVekey and Mazumdar(11)
Rod-disc (push test)	Polyester (cryslic 189)	Surface-coated E-glass	-	Shear	1000	Norman et. al (RAPRA report)19
Rod-disc (push test)	Polyester (Paraplex + p 43)	E-glass acetone cleaned	-	Shear	605	21
"	"	Vinyl Trichlorosilane	-	Shear	680	21
Trapezoidal fibre	"	acetone cleaned	-	Shear	1000	21
"	Epoxy(Epon 828)	"	-	Shear	3000 to 3500	21
Curved Neck method	Polyester (selectron 5026)	E-glass/Heat cleaned	-	Tension	750	21
Curved Neck	"	2% A 172 in Polymer	-	Tension	1220	21
"	Epoxy(Epon 828)	E-glass/Toluene cleaned	-	Tension	1540	21

TABLE 2 : INTERFACIAL SHEAR-STRENGTH FOR POLYESTER - E-GLASS ROVING (PRESENT WORK)

System	Curing condition	Mean inter-facial shear strength	Standard deviation
1. Polyester/E-glass roving (Silane) Rate of cross head movement = 0.01 cm/mt	25°C/72 Hrs.	1180 psi	(0.185)
2. " , 0.05 cm/mt	25°C/72 Hrs.	1696	(0.237)
3. " , 0.01 cm/mt	25°C/72 Hrs.	2300	(0.251)
4. " , 0.01 cm/mt	45°C/24 Hrs.	2640	(0.260)
5. " , 0.01 cm/mt	75°C	3000	(0.27)

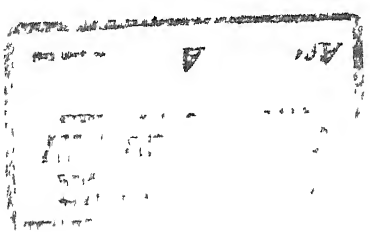

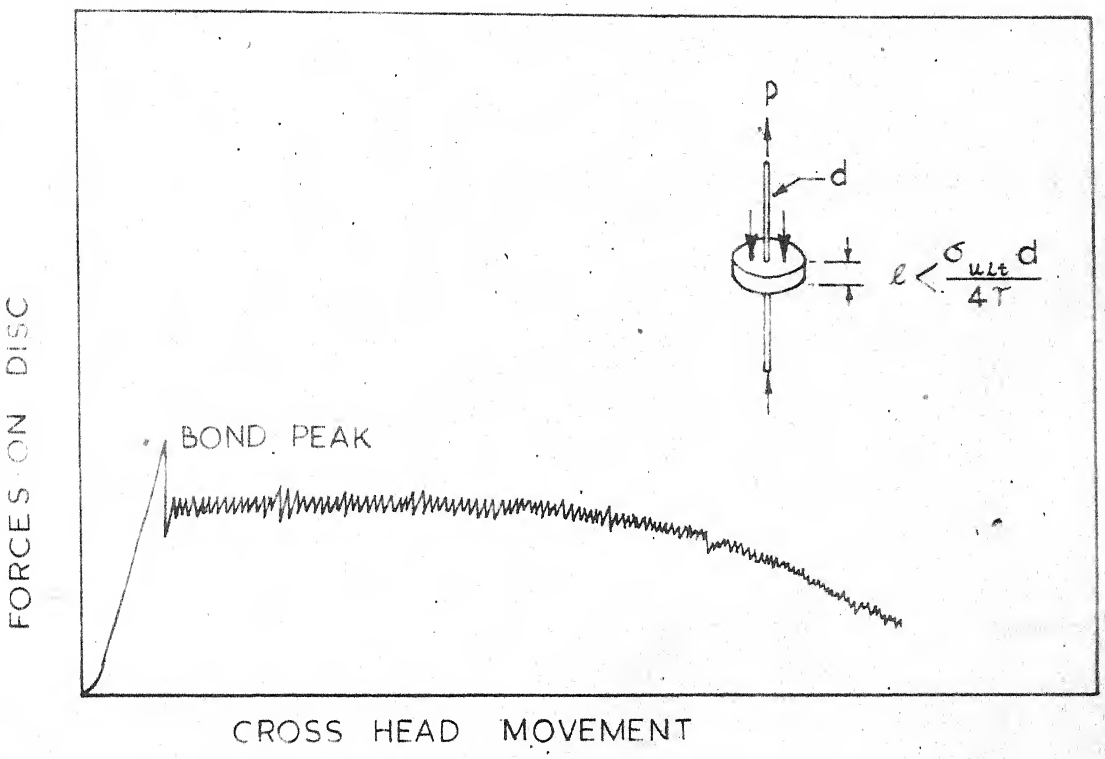

FIG. 1 – TYPICAL LOAD – DISPLACEMENT CURVE FOR ROD DISC. JOINT STRENGTH SPECIMEN.

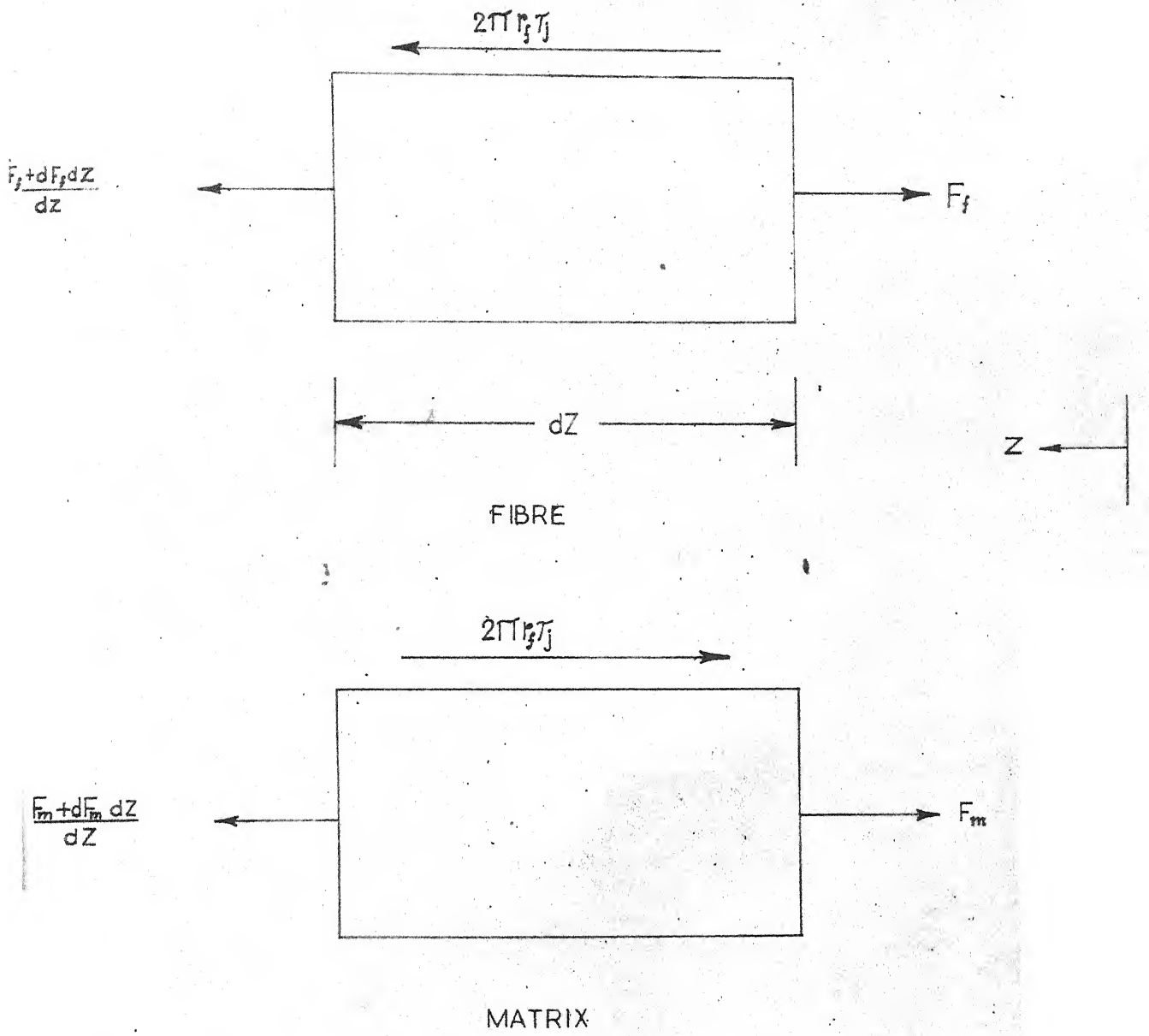

FIG. 2_FORCES ACTING AS AN ELEMENT OF THE FIBRE AND THE MATRIX AT THE INTERFACE

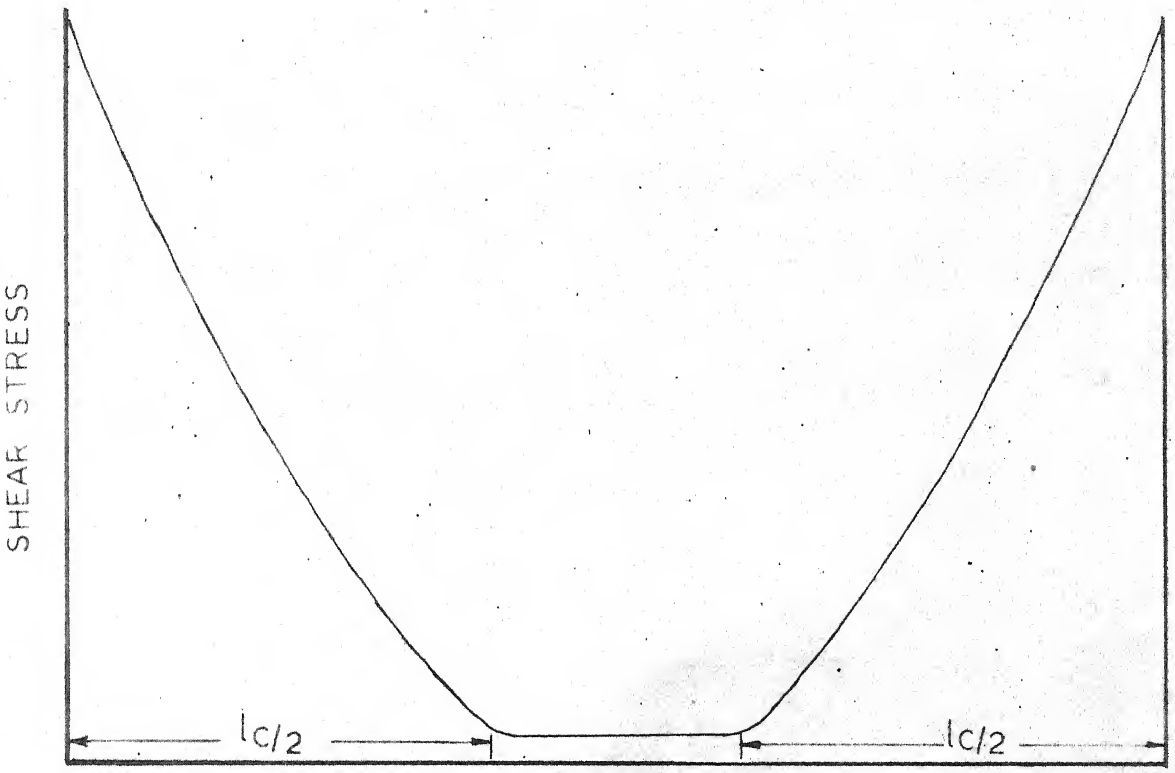

l_c = CRITICAL LENGTH OF FIBRE

FIG.3_THEORETICAL VARIATION OF SHEAR STRESS

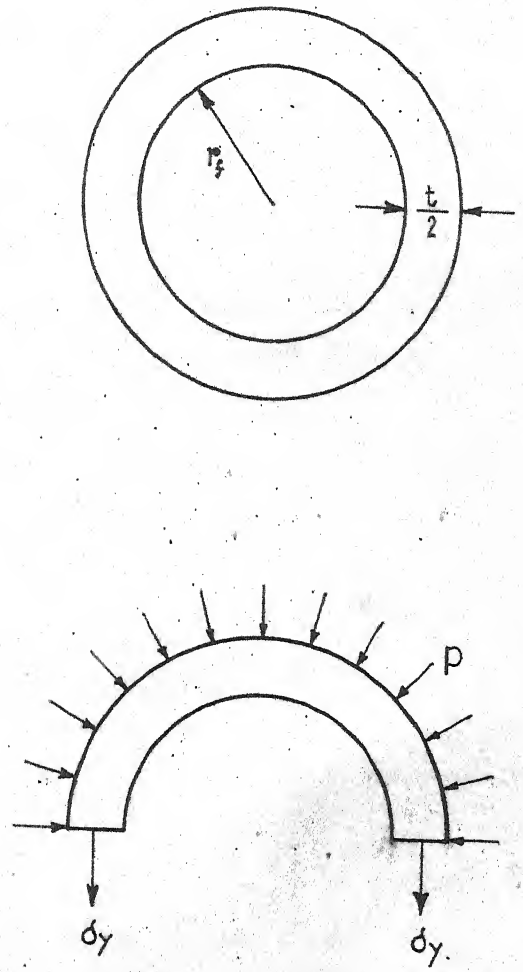

FIG. 4 _ MAXIMUM STRESSES ACTING ON A "THIN CYLINDER" OF THE MATRIX.

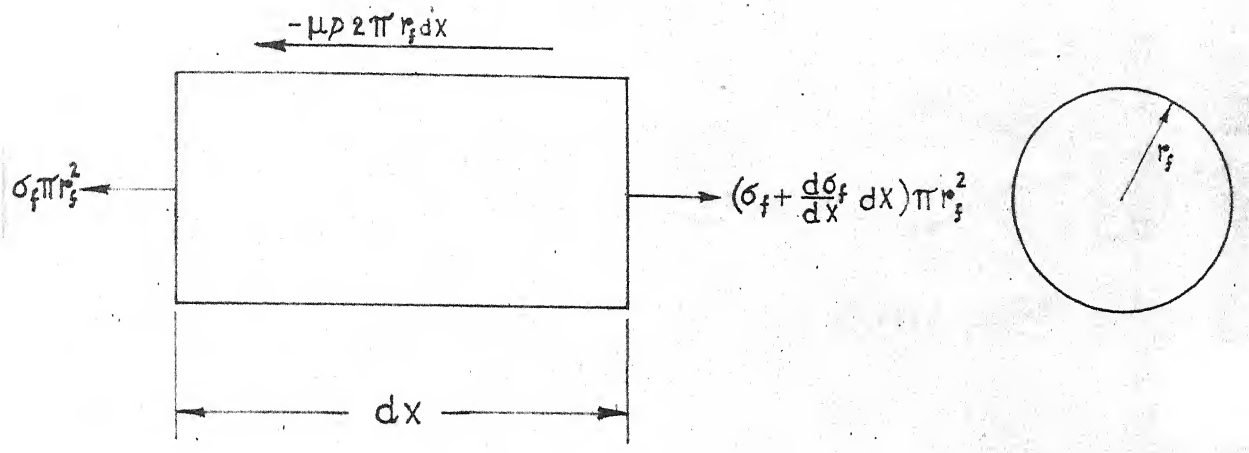

FIG. 5 _ FORCES ACTING ON AN ELEMENT OF A FIBRE.

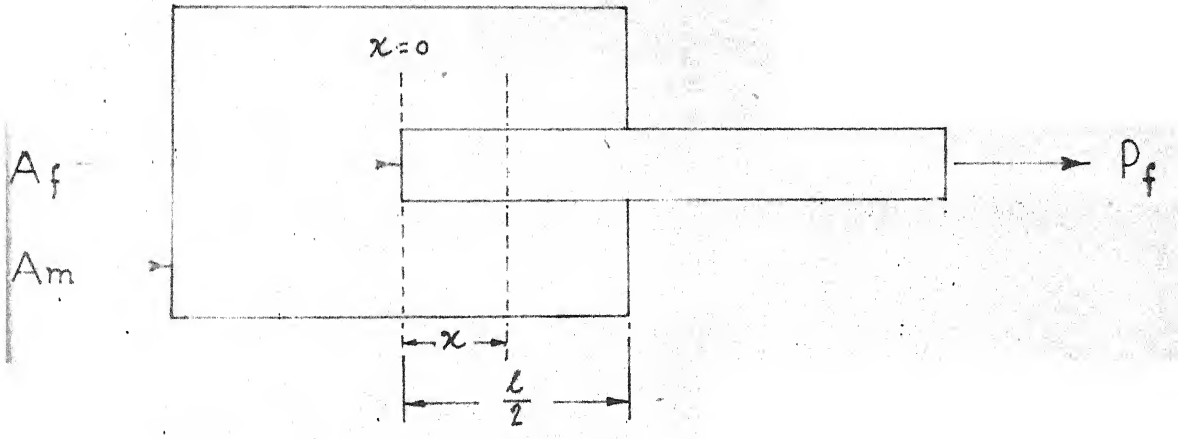

FIG. 6 _ A PULL - OUT TEST CONFIGURATION (LAWRENCE)

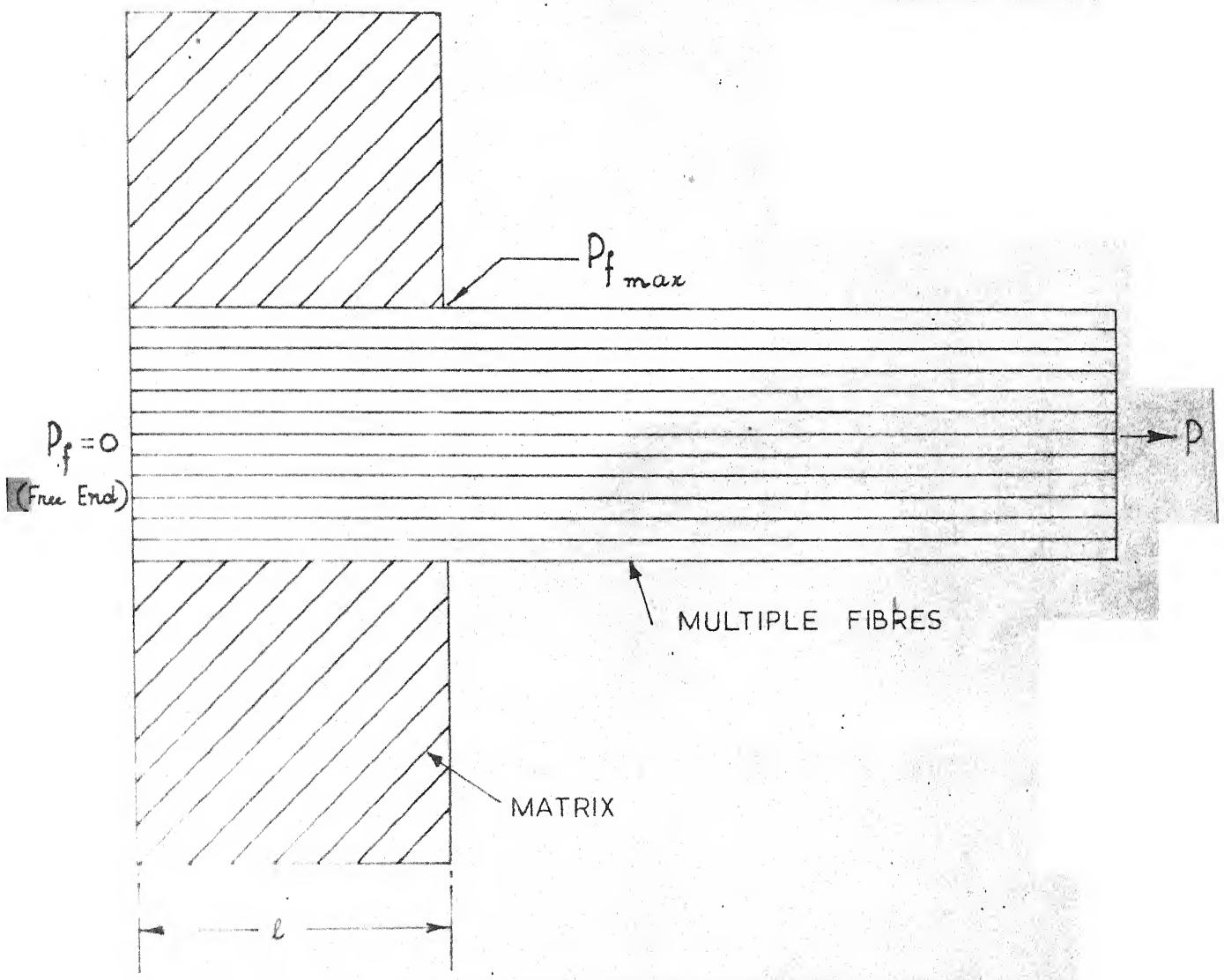

FIG. 7_ PROPOSED PULL-OUT TEST CONFIGURATION

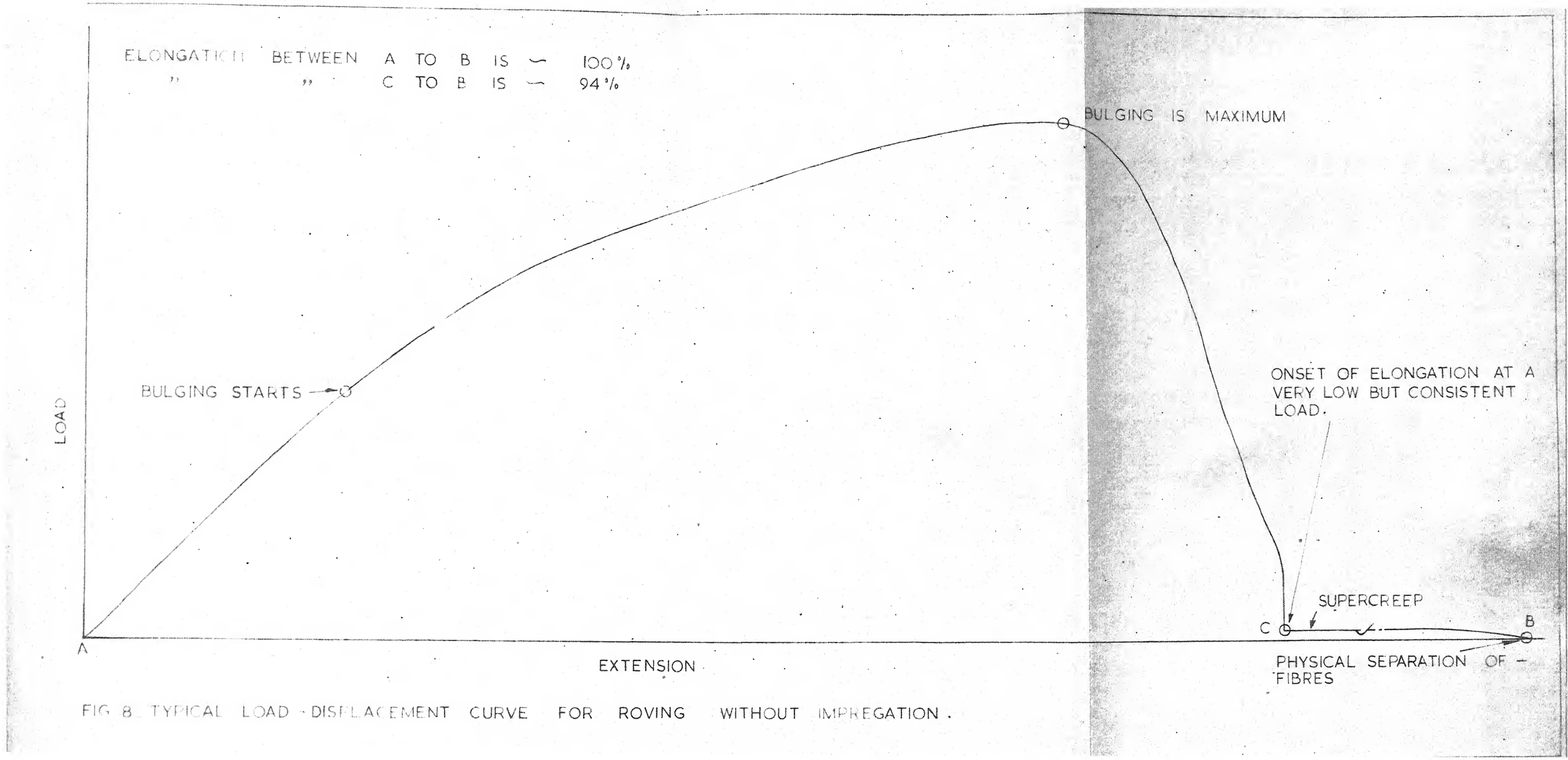

FIG 8 TYPICAL LOAD - DISPLACEMENT CURVE FOR ROVING WITHOUT IMPREGATION.

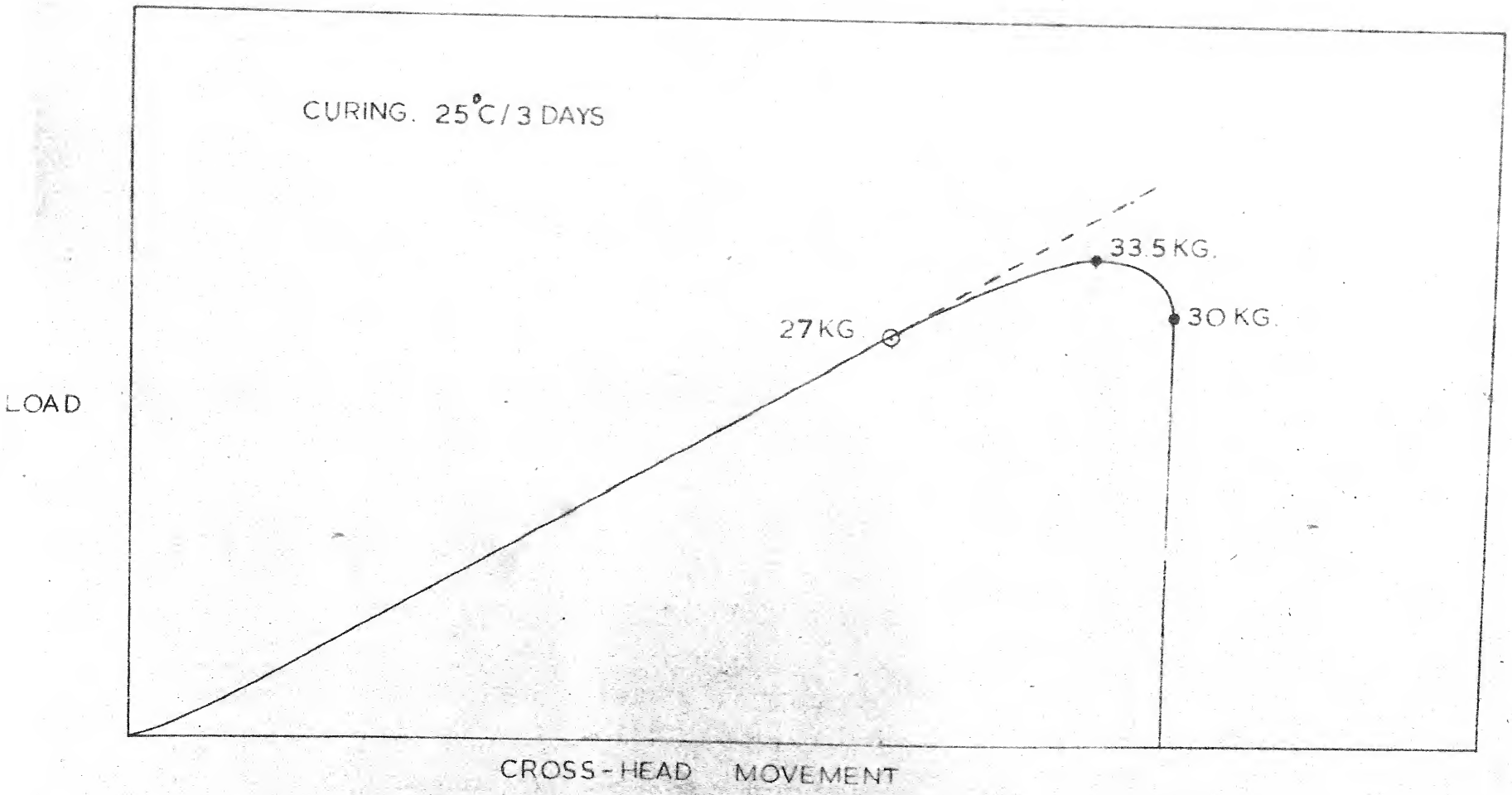

FIG. 9 _ TYPICAL LOAD DISPLACEMENT CURVE FOR DEBONDING AND PULL OUT IN A MULTI-FIBRE SYSTEM. (PRESENT WORK)

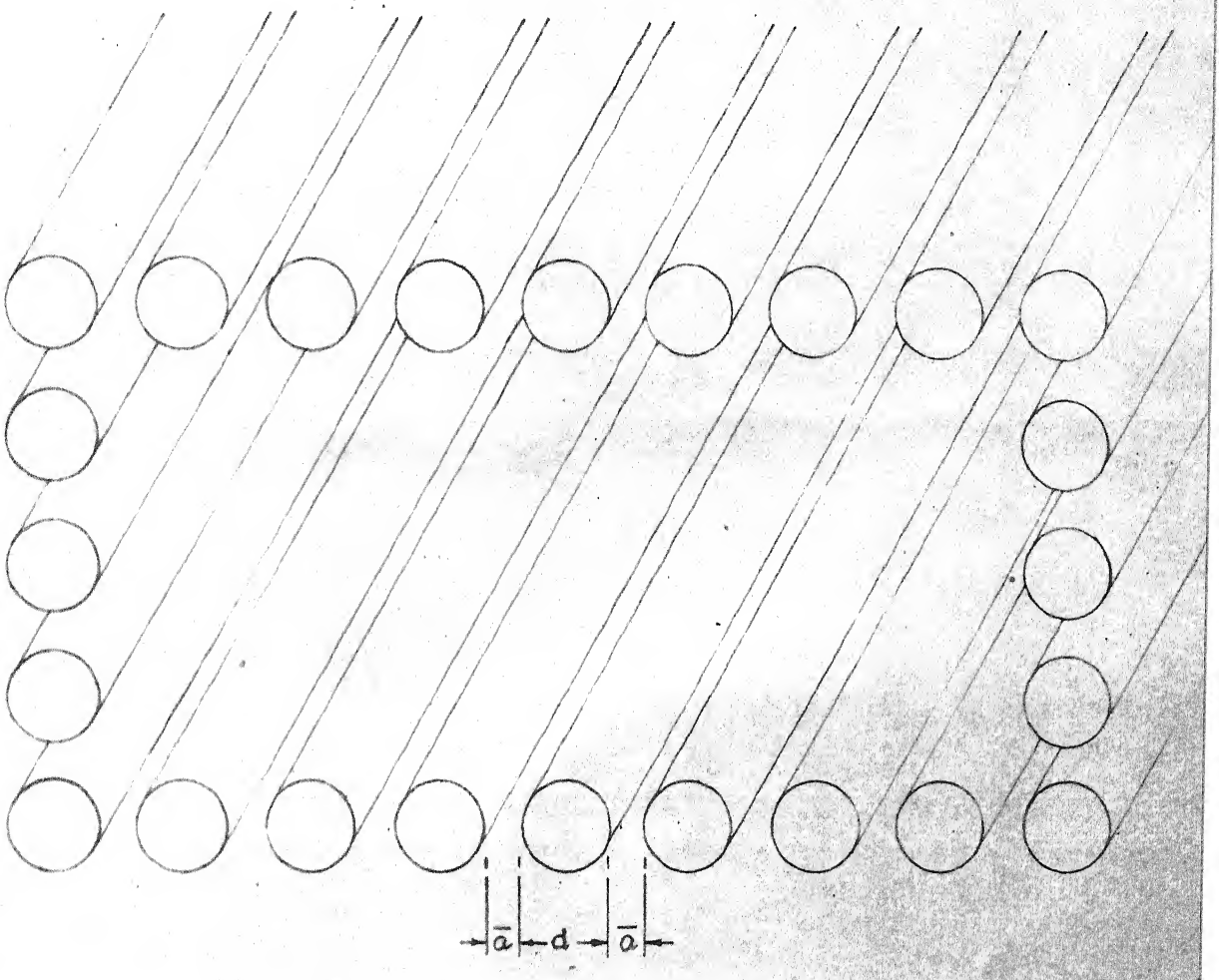

FIG 10 - SHEAR SURFACE FOR THE MULTIPLE FIRER SYSTEM - ONLY THE OUTER FIRERS ARE PRESENTED IN THE FIG.

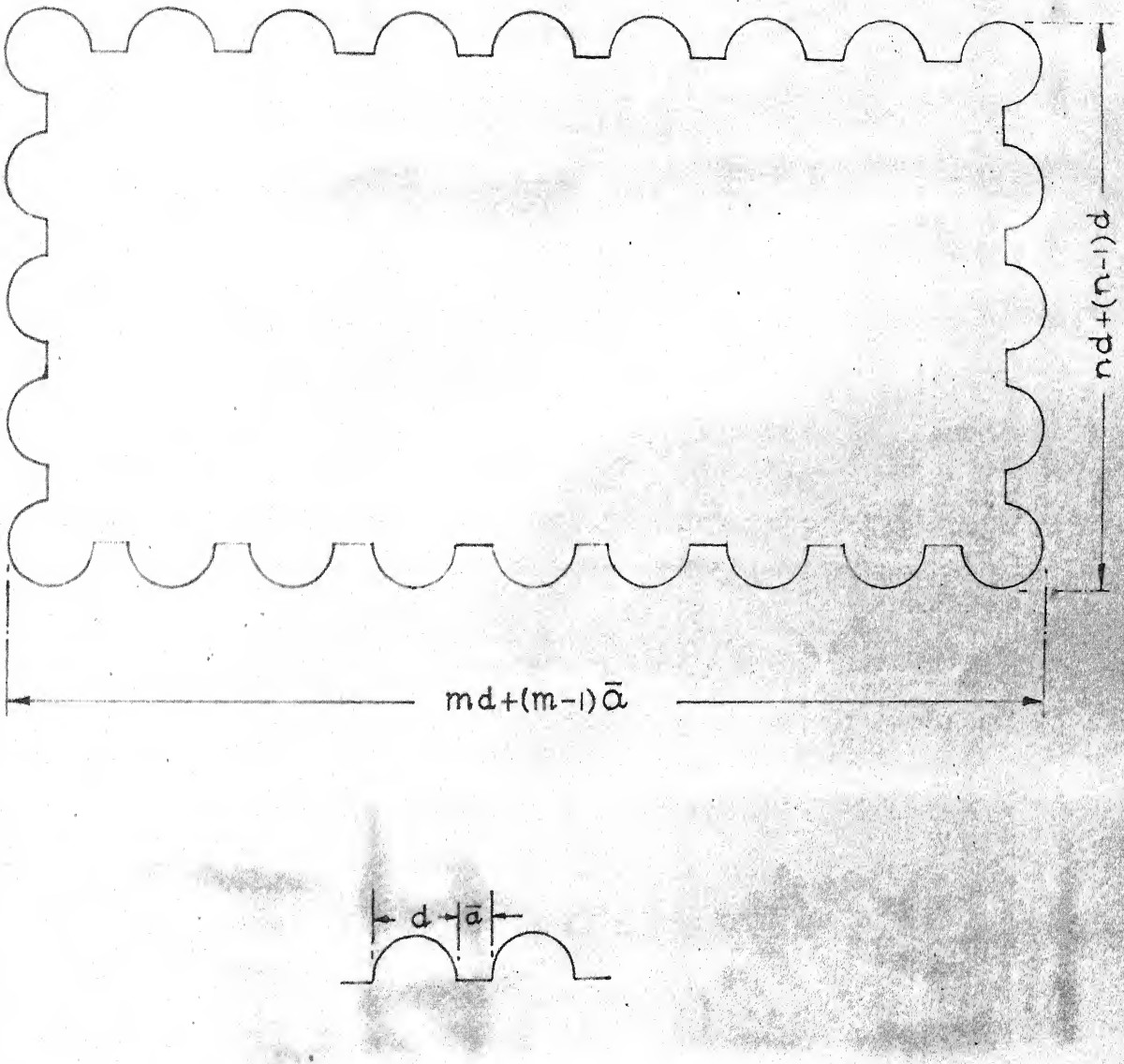

FIG.11_END VIEW OF THE SHEAR SURFACE (FROM FIG.10)

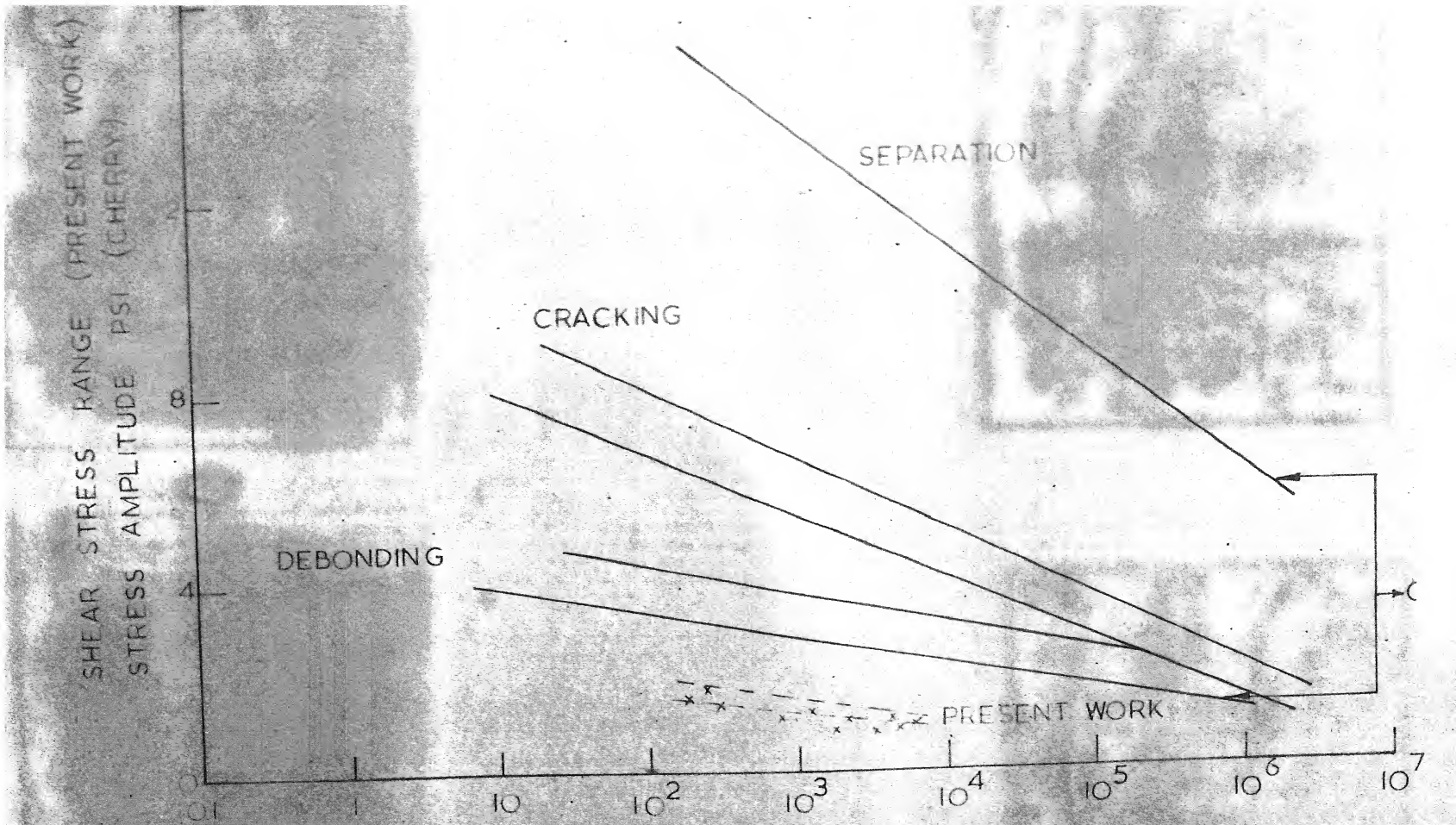

FIG 12_DEPENDENCE OF NUMBER OF CYCLES TO SPECIFIED FAILURE PROCESS APPLIED LOAD.

Plate 1
Cylindrical split mold

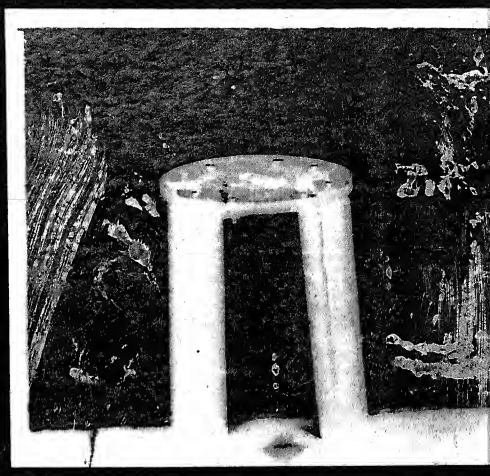

Plate 2
Molding Table

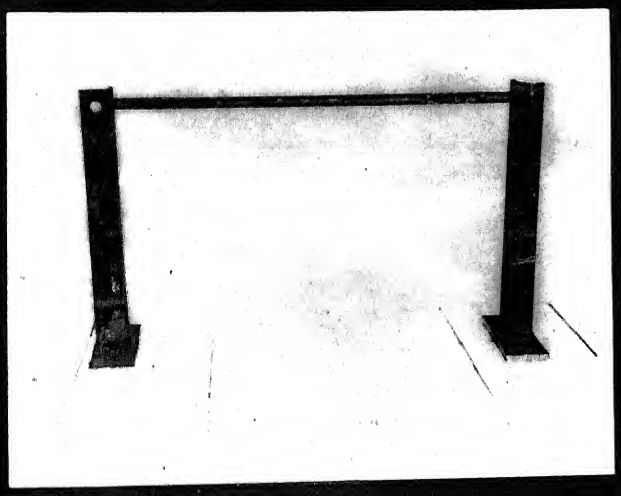

Plate 3
Stand

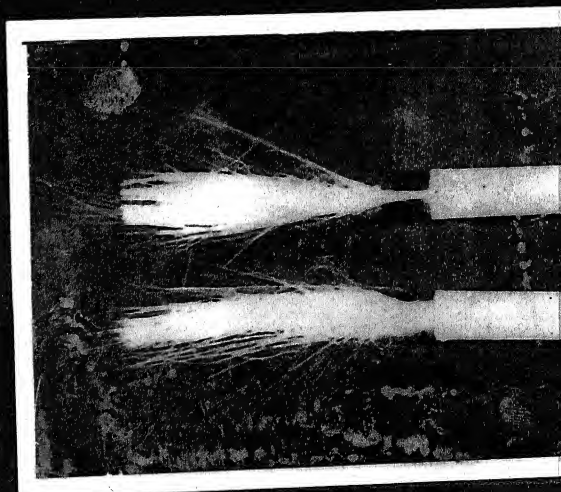

Plate 4
Bulging of fibres

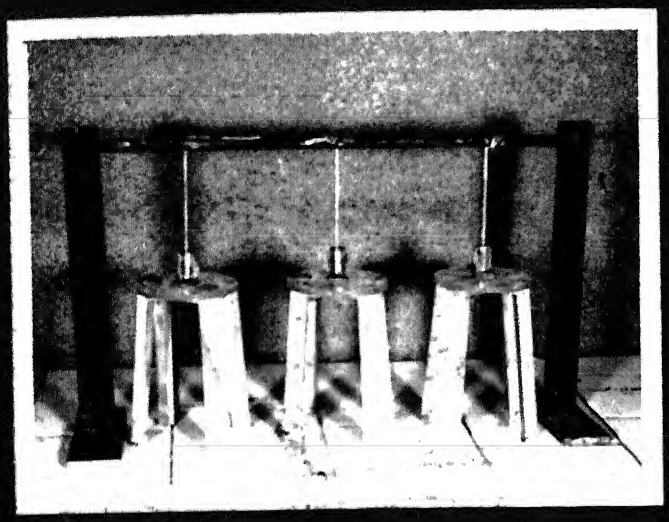

Plate 5

Mold Assembly ready for casting

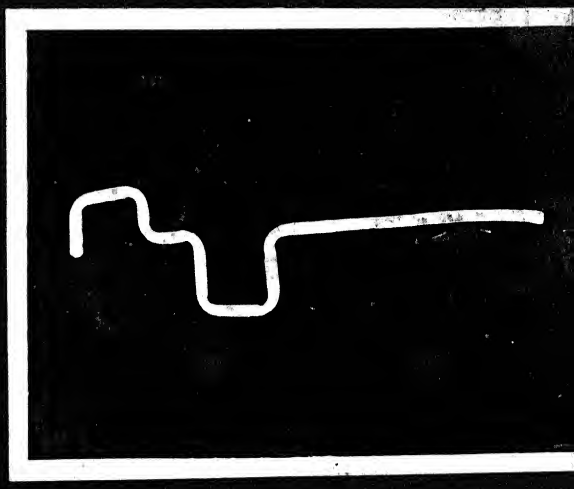

Plate 6

Stirrer

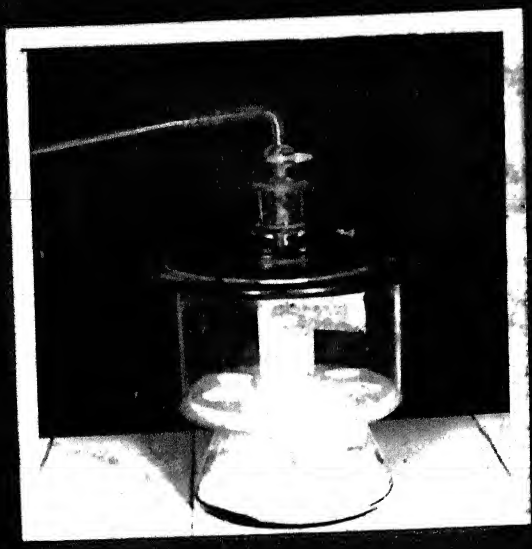

Plate 7

Removal of air bubble from resin in an evacuated Chamber.

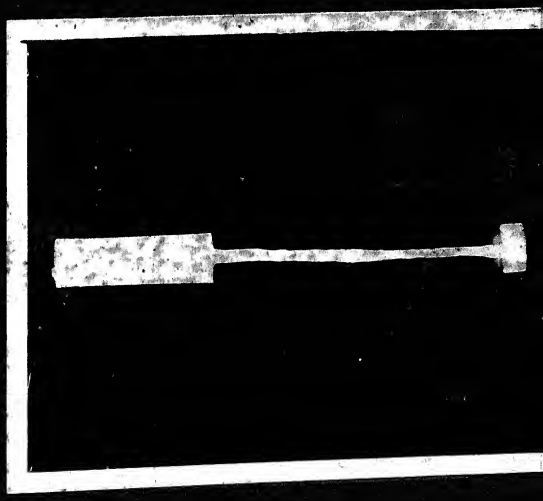

Plate 8

Pull-out specimen, ready for testing

Plate 9.
Roving inside Dessicator

Plate 10
Close up view of debonded a
pulled out surface

Plate 11
Post-cure Preservation
of specimens

Plate 12
Both end cast specimen
(unimpregnated)